

Analysis of the adsorption of Hg^{2+} , Ni^{2+} and Cu^{2+} on chitosan hydrogels

Billy Alberto Ávila-Camacho¹  and Norma Aurea Rangel-Vázquez^{1*} 

¹*Departamento de Posgrado e Investigación, Instituto Tecnológico de Aguascalientes – TecNM, Aguascalientes, AGS, México*

**norma.rv@aguascalientes.tecnm.mx*

Abstract

Chitosan-based adsorbents have high efficiency in removing heavy metals from water. In this study, the adsorption of Hg^{2+} , Ni^{2+} and Cu^{2+} onto chitosan/glutaraldehyde hydrogels were analyzed using the semi-empirical method PM3. Based on thermodynamic analysis of these systems, the adsorption processes were spontaneous, exothermic and highly stable, because all the values of the Gibbs free energy, the enthalpy of formation and the binding energy were negative, on the other hand, each of the systems were analyzed using electrostatic potential maps, where it was observed that the functional groups amino (NH_2) and hydroxyl (OH) are the main active sites of the adsorbent. Through an FTIR analysis, the correct cross-linking between chitosan and glutaraldehyde was confirmed, as well as the union of the different cations on the surface of the adsorbent.

Keywords: *adsorption, chitosan, glutaraldehyde, heavy metals, hydrogel.*

How to cite: Ávila-Camacho, B. A., & Rangel-Vázquez, N. A. (2024). Analysis of the adsorption of Hg^{2+} , Ni^{2+} and Cu^{2+} on chitosan hydrogels. *Polímeros: Ciência e Tecnologia*, 34(3), e20240035. <https://doi.org/10.1590/0104-1428.20240053>

1. Introduction

Treatment of polluted water is a very important issue for the society because it is currently required to improve its quality to minimize the negative impacts on these ecosystems and human health. Water quality has been mainly affected by the industrialization of developed countries, as well as a significant increase in the world's population. There are different types of contaminants as, dyes, organic matter, pharmaceutical compounds, heavy metals, among others^[1]. However, heavy metals are the contaminants that cause the greatest concern, since they are highly toxic even in low concentrations, in addition, they are not biodegradable, so their persistence in water could last for a long time^[2]. Heavy metals such as mercury (Hg), nickel (Ni), copper (Cu), zinc (Zn), lead (Pb) and iron (Fe) have densities greater than 5 gr/cm³^[3]. They have different applications at industrial level^[4]. However, heavy metals can cause different toxicity symptoms^[5]. For this reason, it is necessary to remove heavy metals from water.

Adsorption processes is a physicochemical process in which a substance present in a mobile phase adheres to the surface of a solid material. Different studies have confirmed the efficiency of this process in the single and multicomponent removal of heavy metals^[6,7]. Chitosan is an insoluble linear polycationic polymer due to its bonds formed by hydrogen bonds. This polymer is highly biocompatible, low cost, biodegradable and can be easily chemically modified, which is why it has received great attention as a promising material for various processes including as adsorbent in the treatment of heavy metals^[8,9]. Hydrogels are defined as three-dimensional networks composed by polymers

(e.g., chitosan) that can swell and absorb a certain volume of water into their structure. These materials are made up of various polymeric molecules of a hydrophilic nature, which can be cross-linked through chemical bonds, ionic interactions, or hydrogen bonds.

The swelling capacity of hydrogels is mainly due to the hydrophilic functional groups found within the polymeric network that constitutes the hydrogel, which allows it to absorb and retain large amounts of water, up to 400 times its original weight^[10,11]. There are several techniques adopted for the preparation of hydrogels. Specifically, chemical cross-linking involves the use of a cross-linking agent to join two polymer chains. Chemical crosslinking can be applied to natural polymers (chitosan, alginate, carboxymethylcellulose), which is achieved through the reaction of their functional groups (OH , COOH , NH_2), with cross-linkers such as aldehyde (glutaraldehyde), so this type of cross-linking is permanent^[11,12].

Several investigations have used chitosan hydrogel as an adsorbent in monocomponent systems or in the form of beads^[13], which leads to several disadvantages, for example, a smaller adsorption surface, difficulty in controlling the size, less flexibility and difficulty in scaling up. On the other hand, the addition of graphene oxide^[14] or carbon nanotubes functionalized with chitosan^[15] increase the synthesis costs of chitosan-based adsorbents. This study proposes the use of chitosan hydrogels cross-linked only with glutaraldehyde to simultaneously remove 3 heavy metals from aqueous solutions, reducing the high costs in the synthesis of the

material by drying it at room temperature, reducing the risk of degradation and eliminating the formation of secondary products such as aldehydes and ketones by avoiding the use of sodium hydroxide in the synthesis.

On the other hand, simulation and computational modeling are used for the prediction and optimization of molecular structures, to obtain binding energies and thermodynamic and biological properties, using semi-empirical methods with the objective to optimize the synthesis of materials^[16].

The semiempirical PM3 method has been used to identify evidence for the proposed kinetic models, as well as to explain the adsorption of heavy metals on polymeric materials. On the other hand, quantitative structure-activity relationship (QSAR) parameters are a useful tool to describe the relationships between the biological activity of a molecule and its physicochemical characteristics through its molecular structure^[17]. So, the objective of this work was, the thermodynamic analysis, modeling, simulation, and the experimental adsorption of single and multicomponent systems of heavy metals as, Hg^{2+} , Ni^{2+} and Cu^{2+} in chitosan hydrogels crosslinked with glutaraldehyde.

2. Materials and Methods

2.1 Geometry optimization

The computational analyzes were determined on a DELL brand PC with an i7 processor and 16 Gb of RAM. The molecules were analyzed individually and after the adsorption of the ions in the hydrogel using the Hyperchem software. Semi-empirical models combine quantum theory with empirical approximations to describe the electronic structure and properties of molecules, specifically the Parametric method 3 (PM3) was used to optimize and minimize the geometric energy based on the position of each heavy metal ion in the hydrogel. This model is applicable to organic and inorganic molecules with multiple bonds and functional groups and is more computationally efficient than AB initio quantum theory methods, making it suitable for studying large and complex molecular systems. This model is essentially a reparameterization of AM1 using a different parameterization strategy and only two Gaussian functions. The Polak-Ribiere algorithm and 2250 iterations were used with a convergence level of 0.01 kcal/Å mol.

The molecular structures were built according to the Hyperchem software operating manual using the “build” option; then, using the “model” option, the angles and bond distances of each of the complexes were corrected to obtain the optimization geometry, thermodynamic parameters and QSAR. For chitosan, four glucosamine units were studied, where one unit was acetylated to simulate a deacetylation degree of 75%.

2.2 Thermodynamic and QSAR properties, FTIR and electrostatic potential map

The FTIR spectra were obtained from 200 to 4000 cm^{-1} after the optimization geometry, where an analysis of the rotations and vibrations of the systems at room temperature was carried out. The calculated thermodynamic properties were Gibbs free energy (ΔG), binding energy, Enthalpy of formation (ΔH_f) and dipole moment. On the other hand, the calculated QSAR properties were surface area, volume, and polarizability. The electrostatic potential map (EPM) provides a contour plot of a molecule, indicating the sites of highest and lowest electron density.

3. Results and Discussions

3.1 Chitosan/glutaraldehyde hydrogel

Table 1 shows the thermodynamic properties of glutaraldehyde, chitosan, and the hydrogel, where a negative Gibbs free energy is observed for all cases, specifically in the hydrogel of -464.183 Kcal/mol, indicating the spontaneous nature of the crosslinking through the primary amino groups of chitosan and the aldehyde groups of glutaraldehyde.

The values of the binding energy and the enthalpy of formation of the hydrogel were -19,469.414 and -1,470.360 Kcal/mol respectively, which indicated that the hydrogel is highly stable and exothermic^[18]. On the other hand, the dipole moment is higher in the hydrogel, due to the difference in the electronegativities of the C-H, N-H, C-C, C-O and O-H bonds, respectively.

The QSAR properties of glutaraldehyde, chitosan, and the hydrogel are shown in Table 2, where the surface area and volume in the hydrogel is significantly higher, due to chitosan/glutaraldehyde crosslinking from the Schiff bases reaction. On the other hand, the polarizability of the hydrogel is 130.28 Å³, that is, the tendency to generate induced electric dipole moments is greater, causing a fluctuation in the dipole moment of the hydrogel.

Figure 1 shows the FTIR spectra of glutaraldehyde, chitosan, and chitosan/glutaraldehyde hydrogel, respectively. Figure 1a) show the FTIR of glutaraldehyde where, the band show between 3103-2999 cm^{-1} corresponded to the asymmetric stretching of the H-C-H bonds, to 2058 cm^{-1} it was attributed to the stretching of the C=O bonds. The H-C-H scissoring was appreciated at 1375 cm^{-1} and at 1168 cm^{-1} was assigned to the asymmetric stretching of the C-C bonds. The bands located between 784 and 770 cm^{-1} were attributed to the swinging of the CH_2 bonds and finally, the bands at 600-574 and 226 cm^{-1} corresponded to the swinging in and out of plane of the C=O bonds, respectively.

Table 1. Thermodynamic properties.

System	Gibbs free energy (Kcal/mol)	Binding energy (Kcal/mol)	Enthalpy of formation (Kcal/mol)	Dipole moment (Debyes)
Glutaraldehyde	-32,031	-1,475.812	-85.428	1.763
Chitosan	-243,798	-9,322.778	-854.680	5.317
Hydrogel (CG)	-464,183	-19,469.414	-1,470.36	5.430

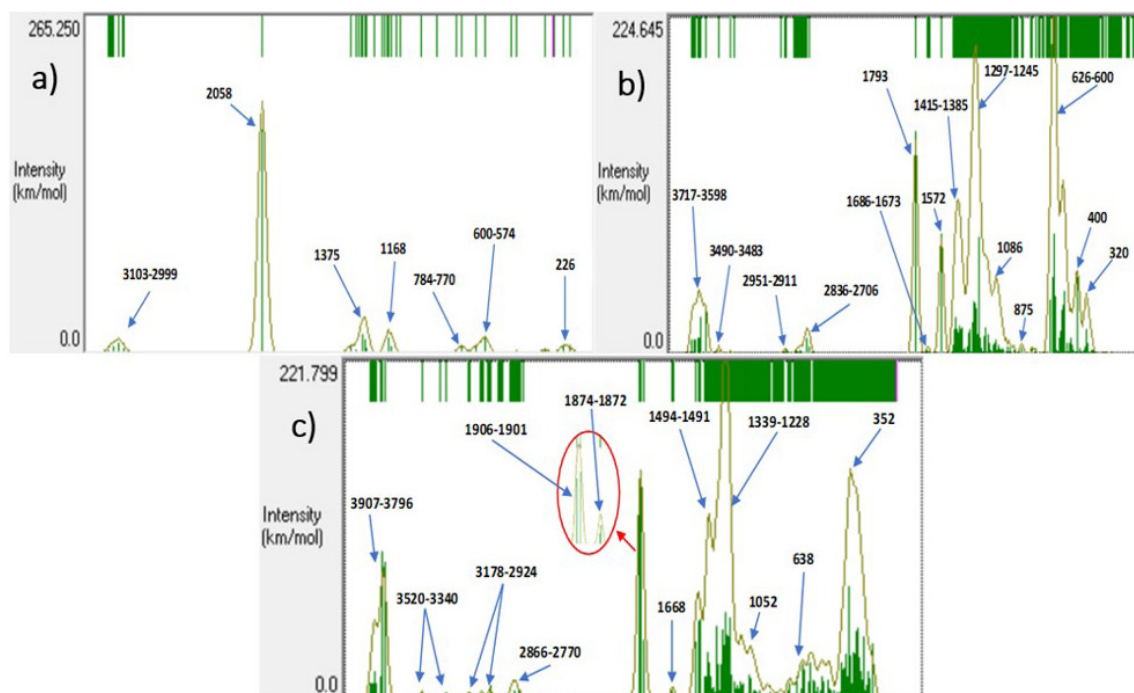


Figure 1. FTIR spectra of the optimized structures were, (a) glutaraldehyde, (b) chitosan, (c) hydrogel.

Table 2. QSAR properties.

System	Surface area (Å ²)	Volume (Å ³)	Polarizability (Å ³)
Glutaraldehyde	316.69	388.36	10.12
Chitosan	614.08	1,654.74	61.71
Hydrogel (CG)	1,320.43	3,450.20	130.28

The FTIR of chitosan can be seen in Figure 1b) where the stretching of the O-H bonds of chitosan were located between 3717 and 3598 cm^{-1} , the symmetrical stretching of the amino groups (NH_2) was appreciated at 3490-3483 cm^{-1} . The range of 2951-2911 cm^{-1} was assigned to the symmetric and asymmetric stretching of CH_3 of the residual acetyl group, in the range of 2836 to 2706 cm^{-1} the stretching of the CH_2 bonds of hydroxymethyl and of the CH bonds of chitosan was observed. At 1793 cm^{-1} was attributed to the stretching of the C=O bond of the residual acetyl, while in the region of 1686 and 1673 cm^{-1} was assigned to the NH_2 scissoring. At 1572 cm^{-1} was attributed to the stretching of the acetyl C-N-C bonds. The peak with the highest intensity located between 1297 and 1245 cm^{-1} was assigned to the swinging of the C-O and C-C bonds, and at 1086 cm^{-1} corresponded to the swinging of C-H. At 875 cm^{-1} the stretching of the chitosan C-C bonds was observed and, finally, in the region of 626-600, 400 and 320 cm^{-1} were attributed to the out-of-plane swinging of the OH, NH and NH_2 bonds, respectively^[19].

The FTIR of the hydrogel is observed in Figure 1c), where a displacement and increase in the intensity of the characteristic peak between 3907-3796 cm^{-1} of the stretching of the O-H bonds due to the hydroxyl groups of chitosan is

shown. In 1874 and 1872 cm^{-1} was assigned to the stretching of the C=N bond of the imine groups, which were formed from the Schiff base reactions due to the crosslinking of glutaraldehyde and chitosan^[20].

The electrostatic potential is related to the electronic density, which represent an important descriptor to determine the sites of electrophilic attack and nucleophilic reactions, as well as the interactions of hydrogen bonds. Figure 2 shows the electronic distribution of chitosan, glutaraldehyde, and hydrogel where the electrophilic and nucleophilic regions are red and blue, respectively. Specifically in the hydrogel, the regions with negative electrostatic potential (-0.132 au) were in the oxygen atoms of the chitosan hydroxyl groups (red spheres), which are the most reactive sites for adsorbate binding.

On the other hand, the nitrogen atoms (blue color) of the amino groups also presented a slightly negative electrostatic potential, so they can also undergo an electrophilic attack. Chitosan is highly chelating^[21], that is, it can interact or form coordinate bonds with other ions or ligands. This phenomenon depends on the availability of empty molecular orbitals and the pH of the solution due to the competition of protons with other ions^[22]. For example, in chitosan, amino and hydroxyl groups represent the most reactive functional groups that are responsible for metal ion chelation due to the presence of a lone pair of electrons on the nitrogen and oxygen atoms^[22,23].

3.2 Single and multicomponent adsorption

Table 3 shows the thermodynamic properties of the adsorption systems. The Gibbs free energy (ΔG) was negative for all the systems, where the adsorption of the different

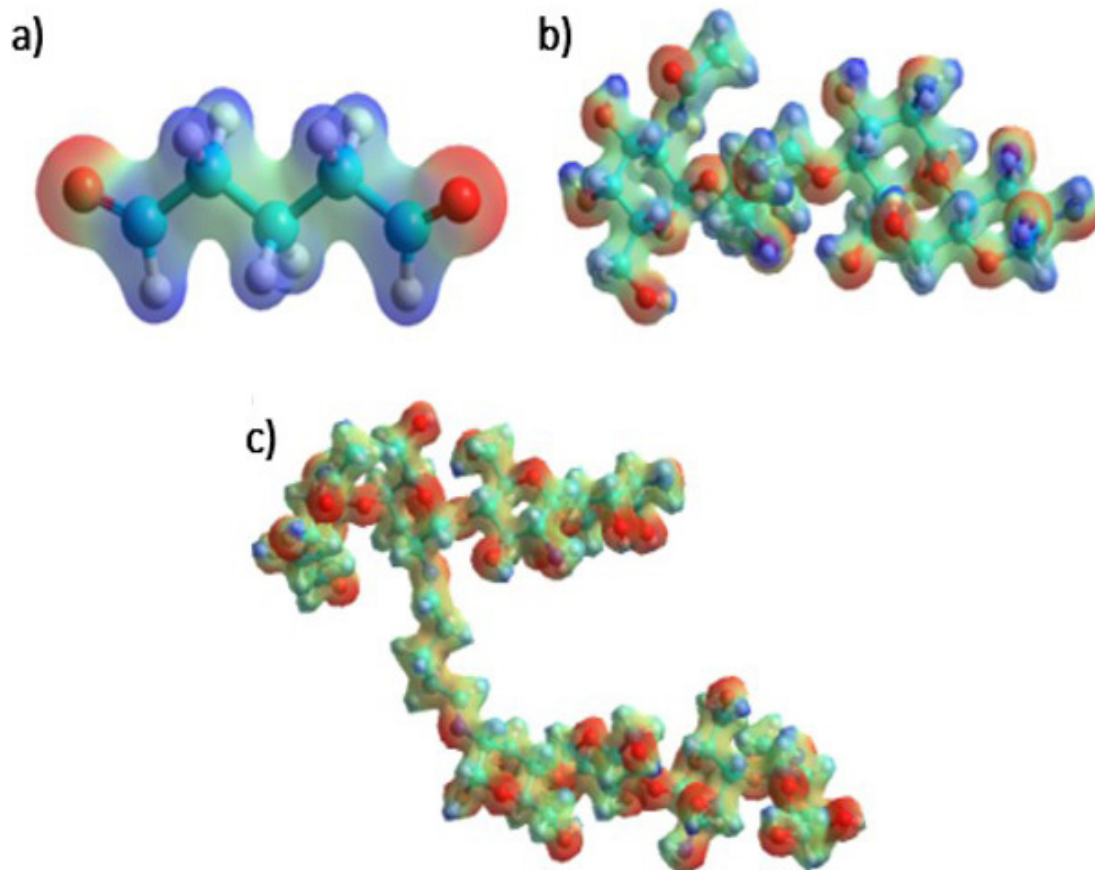


Figure 2. EPM of (a) glutaraldehyde, (b) chitosan, and (c) hydrogel.

Table 3. Thermodynamic properties.

Systems	Gibbs free energy (Kcal/mol)	Binding energy (Kcal/mol)	Enthalpy of formation (Kcal/mol)	Dipole moment (Debyes)
CG-Hg	-464,858	-19,474.032	-1,460.288	8.655
CG-Ni	-488,106	-19,596.771	-1,494.917	10.56
CG-Cu	-469,805	-19,456.644	-1,362.590	9.047
CG-Hg-Ni	-488,774	-19,597.320	-1,480.776	10.737
CG-Hg-Cu	-470,474	-19,455.568	-1,346.824	9.011
CG-Ni-Cu	-493,731	-19,591.584	-1,394.730	12.44
CG-Hg-Ni-Cu	-494,396	-19,583.907	-1,372.360	12.46

cations was spontaneous, in addition, the adsorption occurred due to the lone pair of electrons shared by the NH_2 and OH functional groups generating covalent bonds^[24]. The binding energy and enthalpy determined that the different adsorptions were stable and exothermic.

Finally, the dipole moment was related to electronegativity, that is, the greater the difference in electronegativities between two atoms in a molecule, the greater the dipole moment and, therefore, the polarity. Thus, in the different adsorptions, a higher dipole moment was observed due to the C-O, C-N, O-H and N-H bonds, which presented higher electronegativities differences compared to the rest of the

bonds. Specifically, in the CG-Ni single system, a dipole moment of 10.56 debyes was generated, higher than that of the CG-Cu and CG-Hg systems with 9.047 and 8.655 debyes respectively, in the same way it occurred with the binary systems that contained Ni where the magnitude of the dipole moment was higher, so adsorption may also be higher in such systems^[25].

Table 4 shows the QSAR properties of the single and multicomponent adsorption. In the CG-Hg system was observed that both the surface area and the volume are greater (1,320.61 \AA^2 and 3,493.96 \AA^3 respectively) than the other 2 monocomponent systems CG-Ni and CG-Cu, due to the

Table 4. QSAR properties.

Systems	Surface area (Å ²)	Volume (Å ³)	Polarizability (Å ³)
CG-Hg	1,320.61	3,493.96	130.98
CG-Ni	1,316.25	3,446.97	129.42
CG-Cu	1,316.90	3,454.97	129.41
CG-Hg-Ni	1,305.90	3,484.11	128.72
CG-Hg-Cu	1,320.95	3,508.49	128.70
CG-Ni-Cu	1,299.22	3,438.29	127.84
CG-Hg-Ni-Cu	1,303.71	3,492.33	127.14

volume of the Hg cation of 96.74 Å³, while the volume of Ni and Cu is 33.05 and 36.83 Å³, respectively^[26]. On the other hand, the polarizability values indicated that there may be a temporary fluctuation in the dipole moment of the systems in the presence of an electric field.

The binding energies, the dipole moment, the geometry of the heavy metals, as well as the polarizability of each complex allowed to predict the trend described in the study. Based on the previous results it can be inferred that the possible adsorption tendency would be Ni > Cu > Hg in any of the systems, however, the electronegativity of the heavy metal ions must be considered (2, 1.91 and 1.9, for Hg, Ni and Cu respectively)^[27]. If the electronegativity of heavy metal ions is high, the affinity towards the functional groups of the adsorbent will be greater, adsorbing more easily^[28], therefore, the trend could be the following: Hg > Cu > Ni. Hg has an electronegativity of 2, therefore, it will have a greater attraction for the electron pairs donated by the amine and hydroxyl groups of the chitosan structure.^[29] On the other hand, the stability constants of the amine complexes for Hg, Cu and Ni are approximately 1.3x10²³, 1.3x10¹³ and 1.1x10⁸ respectively, the higher the value of the constant, the greater the affinity between the metal and the amine group, which represents a greater stability of the complex so, the values are consistent with the predicted trend.^[30] Besides, both Cu and Ni are considered intermediate acids, the difference is that Cu tends to form complexes with hard bases such as oxygen, while Ni forms complexes with hard bases such as nitrogen, this behavior is decisive in the adsorption capacities of each heavy metal^[31]. The adsorption of Cu is in the middle because the amount of hydroxyl groups is greater in the chitosan structure, while Ni, by preferring the union with the groups containing nitrogen, is adsorbed less, due to the amount of amine groups present in the chitosan chains is lower because a significant part of said groups are converted into imine groups due to cross-linking.

There is no published information yet on the adsorption of these 3 heavy metals in a ternary system using a chitosan hydrogel, however, there are some others in binary systems using chitosan with similar deacetylation degrees, for example, Boddu et al, carried out the adsorption of Ni and Cu using a chitosan-based adsorbent, said polymer had a deacetylation degree ≥75%, the adsorption capacities they obtained were 86.2 and 78.1 mg/g for Cu and Ni respectively where the trend was Cu>Ni.^[32] Kalyani et al synthesized a low molecular weight chitosan-based adsorbent for the removal of Cu and Ni, where the adsorption capacities were

for Cu and Ni of 196.07 and 114.94 mg/g respectively, that is, the trend was Cu>Ni.^[33] Finally, Vieira et al, investigated the adsorption mechanisms of Hg, Cu and Cr using glutaraldehyde cross-linked chitosan hydrogels with a cross-linking degree of 85%, where the adsorption trend obtained was Hg>Cu>Cr.^[34]

Figure 3 shows the FTIR obtained from the adsorption of the ions in the chitosan/glutaraldehyde hydrogel. In the range of 3900 and 3700 cm⁻¹ the stretching of the OH bonds increased, although the small displacements that were appreciated in the adsorptions were due to the fact that the excited atoms of the cations caused greater vibration and therefore a change in their dipole moment^[25], that is, the adsorbates are interacting with the O atoms of the hydroxyl groups of chitosan^[35]. The FTIR indicated a balancing of the NH₂ groups at 1690 and 1660 cm⁻¹. Additionally, slight increases in the intensity of the peaks and displacements were observed in comparison with the hydrogel, indicating that the cations are also interacting with the N atoms through the lone pair electrons shared from such atoms to the empty orbitals of heavy metals^[36].

Specifically, Figure 3a) shows the FTIR of hydrogel-Hg. The band assigned at 1667-1659 cm⁻¹ indicates the swinging (scissoring) of the H-N-H bonds of the amino groups where Hg is bind. The peak at wave number 1492 cm⁻¹ was attributed to the in-plane rocking of the O-H bonds of the hydroxyl groups. The bands assigned at 1375 and 592 cm⁻¹ were attributed to the out-of-plane and in-plane rocking of the hydroxyl group where Hg binds, respectively. On the other hand, the bands located at 1259, and 1150-1089 cm⁻¹ were assigned to C-O and C-C bonds of the chitosan monomers, as well as to the out-of-plane rocking of the H-C-H bonds respectively. The spectrum within the wavenumber of 345-294 cm⁻¹ indicated the out-of-plane equilibrium of the O-H bonds of the hydroxyl groups. Figure 3b) shows the hydrogel-Ni system where, the band assigned at 1690 cm⁻¹ indicated the rocking (scissoring) of the H-N-H bonds of the amino groups where the Ni ion binds. On the other hand, the peak at located at 514 cm⁻¹ was attributed to the in-plane rocking of the hydroxyl group where Ni is bind.

The system hydrogel-Cu is shown in Figure 3c) where, the band located at 3647 cm⁻¹ was attributed to the stretching of the hydroxyl group where the Cu ion is bind. Besides, the band located at wave number 3472 cm⁻¹ was assigned to the symmetric stretching of the amino group where the same metal is bind.

On the other hand, in the band 1684-1655 cm⁻¹ the rocking (scissor) vibrations of the amino groups were assigned, including the group where the Cu cation binds. The binary system of hydrogel-Hg-Ni is shown in Figure 3d) where, the band located at 3689 cm⁻¹ was attributed to the stretching of the O-H bond where the Ni cation binds. The region between 3516 to 3351 cm⁻¹ was assigned to the symmetric (3516-3491 cm⁻¹) and asymmetric (3402 cm⁻¹) stretching vibrations of the amino groups, including those where the Ni and Hg cations were bind. Figure 3e) shows the hydrogel-Hg-Cu where, the band located at 3646 cm⁻¹ was attributed to the stretching vibration of the hydroxyl group where the Cu cation is bind. The bands between 3517 to

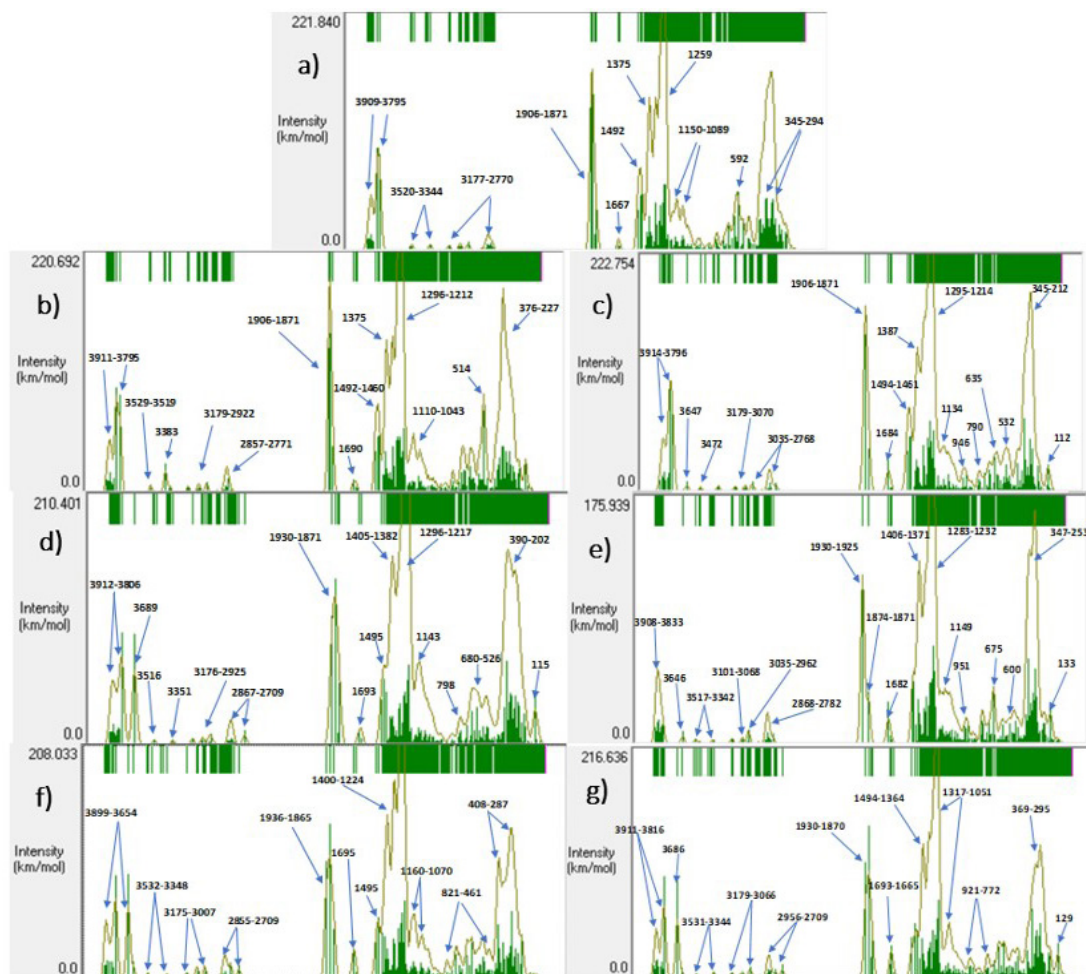


Figure 3. FTIR spectra of the optimized structures where, (a) CG-Hg, (b) CG-Ni, (c) CG-Cu, (d) CG-Hg-Ni, (e) CG-Hg-Cu, (f) CG-Ni-Cu and, (g) CG-Hg-Ni-Cu.

3342 cm^{-1} were assigned to the symmetric stretching vibrations of the amino groups, including those where the binding of heavy metals Hg and Cu occurs, instead, the band located at 1682 cm^{-1} was appreciated to the balancing (scissors) of the free amino groups and those occupied by the heavy metals Hg and Cu. Figure 3f) shows the hydrogel-Ni-Cu system where the peak located between 3695 and 3654 cm^{-1} was attributed to the stretching of the hydroxyl groups where the Ni and Cu cations are bind respectively.

Finally, Figure 3g) shows the multicomponent system hydrogel-Hg-Ni-Cu where, the characteristic bands located between 3911 and 3816 cm^{-1} were assigned to the stretching of the hydroxyl groups, where the Hg and Cu cations are bind, while the band located at 3686 cm^{-1} was localized to the stretching of the same functional group but where Ni binds. The first two low intensity bands within wave numbers 3531 and 3344 cm^{-1} indicated the stretching vibrations of the free amino acid groups and occupied by heavy metals, specifically in 3531, 3491 and 3474 cm^{-1} was assigned to the symmetric stretching of NH_2 where Cu, Hg and Ni bind respectively, while at 3402, 3367 and 3344 cm^{-1} were

attributed to the asymmetric stretching of the amino groups where Ni, Hg and Cu bind respectively.

Figure 4 shows the electronic distribution of the different adsorptions where it is observed that heavy metal ions were adsorbed on the OH and NH_2 functional groups simultaneously (red color) by forming covalent bonds forming an association ring^[36]. The oxygen atoms (red spheres) and nitrogen atoms (blue spheres) presented the negative potential because they have a high electronegativity, that is, they have a greater capacity to attract electrons towards themselves. The carbon atoms (green spheres), mainly the C-C bonds of chitosan, generated neutral electrostatic potentials, that is, there are the electrons that carry out the union of these bonds.

Finally, the positive electrostatic potential was observed mainly around the hydrogen atoms (white sphere), because these atoms have the lowest value of electronegativity compared to the other atoms. In the adsorption systems, a change in the color scale (green-yellow) was observed, mainly in the N and O atoms of the amino and hydroxyl functional groups, respectively, generating a less negative electrostatic

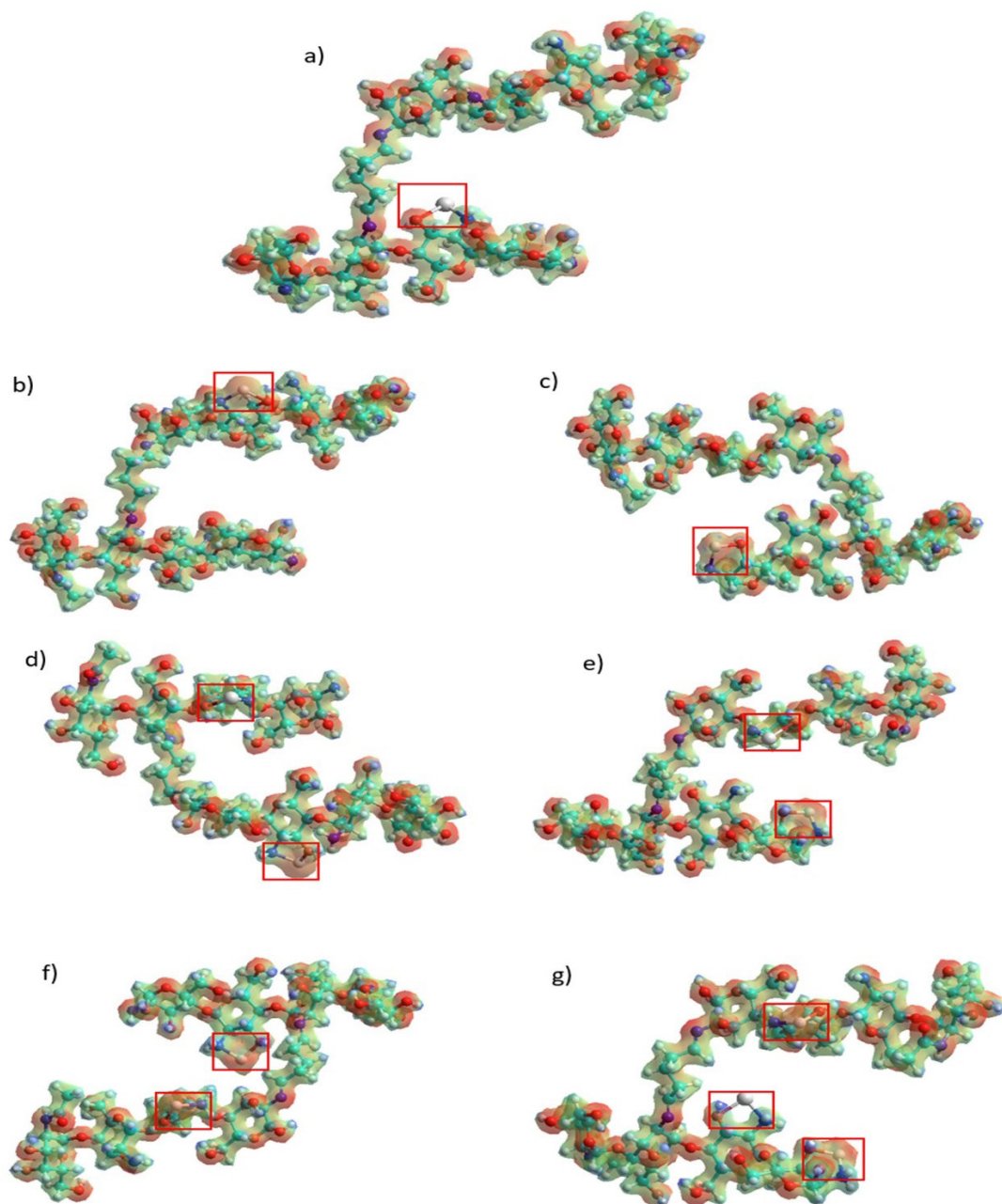


Figure 4. Electrostatic potential maps of optimized structures where, (a) CG-Hg, (b) CG-Ni, (c) CG-Cu, (d) CG-Hg-Ni, (e) CG-Hg-Cu, (f) CG-Ni-Cu and (g) CG-Hg-Ni-Cu.

potential in both groups, which is due to the formation of metal complexes thanks to the donation of lone pairs electrons from N and O to the cations, thus reducing the density of the electron cloud of both functional groups, generating a negative electrostatic potential in the heavy metals^[37].

4. Conclusions

Using computational chemistry methods, adsorption mechanisms can be predicted, as well as the viability

of the processes. In this case, adsorptions occur through the formation of multiple coordination bonds between chitosan functional groups and heavy metal ions, because chitosan-based adsorbent is a strongly chelating agent, therefore adsorption It will depend on several factors, such as electronegativity and polarity. It was appreciated that the adsorptions were spontaneous, stable, and exothermic. In addition, an increase in polarizability was observed specifically in the glutaraldehyde-crosslinked chitosan without the bound ions. The chitosan/glutaraldehyde hydrogel

contains double bonds, which means that these atoms have delocalized electrons, so they are more polarizable, that is, they contribute to a temporary breaking of the dipole moments, causing complementary dipoles in neighboring molecules or ions, so that the adsorbents are attracted to the adsorbates. These studies can be applied to different adsorption systems to determine the viability of the adsorbent and the adsorption system itself.

5. Author's Contribution

- **Conceptualization** – Billy Alberto Ávila-Camacho; Norma Aurea Rangel-Vázquez.
- **Data curation** – Billy Alberto Ávila-Camacho; Norma Aurea Rangel-Vázquez.
- **Formal analysis** – Billy Alberto Ávila-Camacho; Norma Aurea Rangel-Vázquez.
- **Funding acquisition** – NA.
- **Investigation** – Billy Alberto Ávila-Camacho; Norma Aurea Rangel-Vázquez.
- **Methodology** – Billy Alberto Ávila-Camacho; Norma Aurea Rangel-Vázquez.
- **Project administration** – Billy Alberto Ávila-Camacho; Norma Aurea Rangel-Vázquez.
- **Resources** – Billy Alberto Ávila-Camacho; Norma Aurea Rangel-Vázquez.
- **Software** – Billy Alberto Ávila-Camacho; Norma Aurea Rangel-Vázquez.
- **Supervision** – Norma Aurea Rangel-Vázquez.
- **Validation** – Billy Alberto Ávila-Camacho; Norma Aurea Rangel-Vázquez.
- **Visualization** – Billy Alberto Ávila-Camacho; Norma Aurea Rangel-Vázquez.
- **Writing – original draft** – Billy Alberto Ávila-Camacho; Norma Aurea Rangel-Vázquez.
- **Writing – review & editing** – Billy Alberto Ávila-Camacho; Norma Aurea Rangel-Vázquez.

6. Acknowledgements

Billy Alberto Ávila-Camacho thanks to National Council of Humanities, Sciences and Technologies (CONAHCYT) for the Doctorate in Engineering Science 834799 scholarship.

7. References

1. Villarín, M. C., & Merel, S. (2020). Assessment of current challenges and paradigm shifts in wastewater management. *Journal of Hazardous Materials*, 390, 122139. <http://doi.org/10.1016/j.jhazmat.2020.122139>. PMID:32007860.
2. Briffa, J., Sinagra, E., & Blundell, R. (2020). Heavy metal pollution in the environment and their toxicological effects on humans. *Heliyon*, 6(9), e04691. <http://doi.org/10.1016/j.heliyon.2020.e04691>. PMID:32964150.
3. Zamora-Ledezma, C., Negrete-Bolagay, D., Figueroa, F., Zamora-Ledezma, E., Ni, M., Alexis, F., & Guerrero, V. H. (2021). Heavy metal water pollution: a fresh look about hazards, novel and conventional remediation methods. *Environmental Technology & Innovation*, 22, 101504. <http://doi.org/10.1016/j.eti.2021.101504>.
4. Ando, S., & Koide, K. (2011). Development and applications of fluorogenic probes for mercury (II) based on vinyl ether oxymercuration. *Journal of the American Chemical Society*, 133(8), 2556-2566. <http://doi.org/10.1021/ja108028m>. PMID:21294513.
5. Taylor, A. A., Tsuji, J. S., Garry, M. R., McArdle, M. E., Goodfellow, W. L., Jr., Adams, W. J., & Menzie, C. A. (2019). Critical review of exposure and effects: implications for setting regulatory health criteria for ingested copper. *Environmental Management*, 65(1), 131-159. <http://doi.org/10.1007/s00267-019-01234-y>. PMID:31832729.
6. Zeng, X., Zhang, G., Zhu, J., & Wu, Z. (2022). Adsorption of heavy metal ions in water by surface functionalized magnetic composites: a review. *Environmental Science. Water Research & Technology*, 8(5), 907-925. <http://doi.org/10.1039/D1EW00868D>.
7. Arora, R. (2019). Adsorption of heavy metals—a review. *Materials Today: Proceedings*, 18(Pt 7), 4745-4750. <http://doi.org/10.1016/j.matpr.2019.07.462>.
8. Li, Q., Dunn, E. T., Grandmaison, E. W., & Goosen, M. F. (1992). Applications and properties of chitosan. *Journal of Bioactive and Compatible Polymers*, 7(4), 370-397. <http://doi.org/10.1177/088391159200700406>.
9. Cheng, B., Pei, B., Wang, Z., & Hu, Q. (2017). Advances in chitosan-based superabsorbent hydrogels. *RSC Advances*, 7(67), 42036-42046. <http://doi.org/10.1039/C7RA07104C>.
10. Ahmed, E. M. (2015). Hydrogel: Preparation, characterization, and applications: A review. *Journal of Advanced Research*, 6(2), 105-121. <http://doi.org/10.1016/j.jare.2013.07.006>. PMID:25750745.
11. Gulrez, S. K. H., Al-Assaf, S., & Phillips, G. O. (2011). *Hydrogels: methods of preparation, characterization and applications*. In A. Carpi (Ed.), *Progress in molecular and environmental bioengineering—from analysis and modeling to technology applications* (pp. 117150). Italy: InTech. <http://doi.org/10.5772/24553>.
12. Silos-Llamas, A. K., Durán-Jiménez, G., Hernández-Montoya, V., Montes-Morán, M. A., & Rangel-Vázquez, N. A. (2020). Understanding the adsorption of heavy metals on oxygen-rich biochars by using molecular simulation. *Journal of Molecular Liquids*, 298, 112069. <http://doi.org/10.1016/j.molliq.2019.112069>.
13. Ngah, W. S. W., Ab Ghani, S., & Kamari, A. (2005). Adsorption behaviour of Fe (II) and Fe (III) ions in aqueous solution on chitosan and cross-linked chitosan beads. *Bioresource Technology*, 96(4), 443-450. <http://doi.org/10.1016/j.biortech.2004.05.022>. PMID:15491825.
14. Medina, R. P., Nadres, E. T., Ballesteros, F. C., Jr., & Rodrigues, D. F. (2016). Incorporation of graphene oxide into a chitosan-poly (acrylic acid) porous polymer nanocomposite for enhanced lead adsorption. *Environmental Science. Nano*, 3(3), 638-646. <http://doi.org/10.1039/C6EN00021E>.
15. Kim, M. K., Sundaram, K. S., Iyengar, G. A., & Lee, K.-P. (2015). A novel chitosan functional gel included with multiwall carbon nanotube and substituted polyaniline as adsorbent for efficient removal of chromium ion. *Chemical Engineering Journal*, 267, 51-64. <http://doi.org/10.1016/j.cej.2014.12.091>.
16. Atangana, E., & Oberholster, P. J. (2020). Mathematical modeling and stimulation of thermodynamic parameters for the removal of Cr6+ from wastewater using chitosan cross-linked glutaraldehyde adsorbent. *Alexandria Engineering Journal*, 59(4), 1931-1939. <http://doi.org/10.1016/j.aej.2019.12.012>.
17. Costa-Júnior, E. S., Barbosa-Stancioli, E. F., Mansur, A. A. P., Vasconcelos, W. L., & Mansur, H. S. (2009). Preparation and characterization of chitosan/poly (vinyl alcohol)

- chemically crosslinked blends for biomedical applications. *Carbohydrate Polymers*, 76(3), 472-481. <http://doi.org/10.1016/j.carbpol.2008.11.015>.
18. Mirzaei, E. B., Ramazani, A. S. A., Shafiee, M., & Danaei, M. (2013). Studies on glutaraldehyde crosslinked chitosan hydrogel properties for drug delivery systems. *International Journal of Polymeric Materials and Polymeric Biomaterials*, 62(11), 605-611. <http://doi.org/10.1080/00914037.2013.769165>.
 19. Li, B., Shan, C.-L., Zhou, Q., Fang, Y., Wang, Y.-L., Xu, F., Han, L.-R., Ibrahim, M., Guo, L.-B., Xie, G.-L., & Sun, G.-C. (2013). Synthesis, characterization, and antibacterial activity of cross-linked chitosan-glutaraldehyde. *Marine Drugs*, 11(5), 1534-1552. <http://doi.org/10.3390/md11051534>. PMID:23670533.
 20. Galan, J., Trilleras, J., Zapata, P. A., Arana, V. A., & Grande-Tovar, C. D. (2021). Optimization of chitosan glutaraldehyde-crosslinked beads for reactive blue 4 anionic dye removal using a surface response methodology. *Life*, 11(2), 85. <http://doi.org/10.3390/life11020085>. PMID:33504022.
 21. Gamage, A., & Shahidi, F. (2007). Use of chitosan for the removal of metal ion contaminants and proteins from water. *Food Chemistry*, 104(3), 989-996. <http://doi.org/10.1016/j.foodchem.2007.01.004>.
 22. Guibal, E. (2004). Interactions of metal ions with chitosan-based sorbents: a review. *Separation and Purification Technology*, 38(1), 43-74. <http://doi.org/10.1016/j.seppur.2003.10.004>.
 23. Guibal, E., Vincent, T., & Navarro, R. (2014). Metal ion biosorption on chitosan for the synthesis of advanced materials. *Journal of Materials Science*, 49(16), 5505-5518. <http://doi.org/10.1007/s10853-014-8301-5>.
 24. Alsamman, M. T., & Sanchez, J. (2021). Recent advances on hydrogels based on chitosan and alginate for the adsorption of dyes and metal ions from water. *Arabian Journal of Chemistry*, 14(12), 103455. <http://doi.org/10.1016/j.arabjc.2021.103455>.
 25. González, A. J., & Vázquez, N. A. R. (2023). PM3 semi-empirical method and Monte Carlo simulation application on pesticides adsorption on SWCNT. *Colloid and Interface Science Communications*, 53, 100699. <http://doi.org/10.1016/j.colcom.2023.100699>.
 26. Bader, R. F., Carroll, M. T., Cheeseman, J. R., & Chang, C. (1987). Properties of atoms in molecules: atomic volumes. *Journal of the American Chemical Society*, 109(26), 7968-7979. <http://doi.org/10.1021/ja00260a006>.
 27. Allred, A. L. (1961). Electronegativity values from thermochemical data. *Journal of Inorganic and Nuclear Chemistry*, 17(3-4), 215-221. [http://doi.org/10.1016/0022-1902\(61\)80142-5](http://doi.org/10.1016/0022-1902(61)80142-5).
 28. Zhu, H., Chen, S., & Luo, Y. (2023). Adsorption mechanisms of hydrogels for heavy metal and organic dyes removal: A short review. *Journal of Agriculture and Food Research*, 12, 100552. <http://doi.org/10.1016/j.jafr.2023.100552>.
 29. Li, K., & Xue, D. (2006). Estimation of electronegativity values of elements in different valence states. *The Journal of Physical Chemistry A*, 110(39), 11332-11337. <http://doi.org/10.1021/jp062886k>. PMID:17004743.
 30. Basolo, F., & Pearson, R. G. (1967) *Mechanisms of inorganic reactions a study of metal complexes in solution*. New York: John Wiley and Sons, Inc.
 31. Pearson, R. G. (1963). Hard and soft acids and bases. *Journal of the American Chemical Society*, 85(22), 3533-3539. <http://doi.org/10.1021/ja00905a001>.
 32. Boddu, V. M., Abburi, K., Randolph, A. J., & Smith, E. D. (2008). Removal of copper (II) and nickel (II) ions from aqueous solutions by a composite chitosan biosorbent. *Separation Science and Technology*, 43(6), 1365-1381. <http://doi.org/10.1080/01496390801940762>.
 33. Kalyani, S., Priya, J. A., Rao, P. S., & Krishnaiah, A. J. S. S. (2005). Removal of copper and nickel from aqueous solutions using chitosan coated on perlite as biosorbent. *Separation Science and Technology*, 40(7), 1483-1495. <http://doi.org/10.1081/SS-200055940>.
 34. Vieira, R. S., Oliveira, M. L. M., Guibal, E., Rodríguez-Castellón, E., & Beppu, M. M. (2011). Copper, mercury and chromium adsorption on natural and crosslinked chitosan films: an XPS investigation of mechanism. *Colloids and Surfaces. A, Physicochemical and Engineering Aspects*, 374(1-3), 108-114. <http://doi.org/10.1016/j.colsurfa.2010.11.022>.
 35. Jiang, C., Wang, X., Wang, G., Hao, C., Li, X., & Li, T. (2019). Adsorption performance of a polysaccharide composite hydrogel based on crosslinked glucan/chitosan for heavy metal ions. *Composites. Part B, Engineering*, 169, 45-54. <http://doi.org/10.1016/j.compositesb.2019.03.082>.
 36. Yu, K., Ho, J., Mccandlish, E., Buckley, B., Patel, R., Li, Z., & Shapley, N. C. (2013). Copper ion adsorption by chitosan nanoparticles and alginate microparticles for water purification applications. *Colloids and Surfaces. A, Physicochemical and Engineering Aspects*, 425, 31-41. <http://doi.org/10.1016/j.colsurfa.2012.12.043>.
 37. Li, N., & Bai, R. (2005). Copper adsorption on chitosan-cellulose hydrogel beads: behaviors and mechanisms. *Separation and Purification Technology*, 42(3), 237-247. <http://doi.org/10.1016/j.seppur.2004.08.002>.

Received: Jun. 12, 2024

Revised: Aug. 08, 2024

Accepted: Aug. 14, 2024

Supplementary Material

Supplementary material accompanies this paper.

Supplementary Information

This material is available as part of the online article from <https://doi.org/10.1590/0104-1428.20240053>